ORIGINAL ARTICLE

Evaluation of Paranasal Sinus Variations with Computed Tomography

ⓘ **Gülay Güngör**[1], ⓘ **Nazan Okur**[2]

[1]Department of Radiology, Pamukkale University, Denizli, Turkey
[2]Department of Radiology, Süleyman Demirel University, Isparta, Turkey

Abstract

Introduction: Paranasal sinuses are one of the most common anatomical variations in humans. Computed tomography (CT) is an imaging modality used as the gold standard in the evaluation of patients before endoscopic sinus surgery (ESS). This study aims to evaluate the anatomic variations that should be considered before and during the surgical procedure by CT examination and to determine their frequency.

Methods: In this study, the images of patients who were referred to the otorhinolaryngology (ENT) outpatient clinic, considering that they had had sinus pathology and underwent paranasal sinus CT imaging were retrospectively analyzed. A total of 320 patients aged between 15-90 years were evaluated. Non-contrast images obtained by multislice CT were examined. The breakdown of anatomic variations evaluated in CT sections obtained according to these protocols is presented in Table 1.

Results: Of the 300 patients, 151 were male (47.2%) and 169 were female (52.8%). The mean age was 39.8±15.8 years. The most common anatomic variation was agger nasi cell with 86.3% (n=276). The least detected anatomical variations were pneumatized inferior turbinate and bifid inferior turbinate as 0% (n=0), inferior turbinate hypoplasia as 0.3% (n=1), and bifid uncinate process variations as 0.6% (n=2).

Discussion and Conclusion: Considering that a significant portion of the variations identified in this study (such as ICA protrusion and dehiscence, ethmoid roof asymmetry, Onodi cell, atelectatic UP) may lead to significant complications during surgery, it is important to know and describe the appearance of these variations on CT. In our study, significant variation was observed in the sinonasal region, and it was once again emphasized that paranasal sinus CT was very valuable in determining these variations.

Keywords: Computed tomography; endoscopic sinus surgery; paranasal sinus variation.

Paranasal sinuses are the structures with highly complex anatomy that may vary according to the individual and are one of the regions with the most anatomical variations [1,2]. Currently, endoscopic nasal examination and computed tomography (CT) are routinely used to detect the anatomy and pathologies of the nasal cavity and paranasal sinuses [3]. Expanding the limits of endoscopic sinus surgery is parallel to the frequency and experience.

However, the most important factor affecting the outcome of surgery and complication rates is the orientation of the surgeon on the anatomy [2,4].

CT is an imaging modality used as the gold standard in the evaluation of patients before the endoscopic sinus surgery (ESS). With superiority of bone and soft tissue analysis, axial and coronal imaging, and multi-detector devices that have become widespread in recent years, CT has the ability

to reshape and multi-detector quality; plays an important role in the diagnosis, selection of treatment protocols and in determining surgical margins in patients undergoing surgery [2,5,6].

In this study, the anatomic variations in the paranasal sinuses were investigated using CT. This study aimed to evaluate and determine the frequency of the anatomical variations that should be considered to avoid the complications that may occur during the surgical procedure.

Materials and Methods

In this study, the images of the patients who were examined in the otorhinolaryngology (ENT) outpatient clinic and who underwent paranasal sinus CT imaging according to their anamnesis and physical examination findings were examined retrospectively. Patients with previous sinonasal surgery, sinonasal massive polyposis, severe sinus inflammatory disease, congenital major anomaly, fibro-osseous lesion and sinus malignancy were excluded from this study. A total of 320 patients (151 male and 169 female) aged between 15-90 years were evaluated in our study.

The examination was performed using a 6-row Philips Brilliance (Philips Brilliance CT, Philips Medical Systems, the Netherlands) multislice CT. For axial screening, the patient was placed in the supine position. In the axial plane, a non-contrast image was obtained with 3 mm consecutive sections, using 120 kV (kilovolt), 120-200 mA (milliampere) with a plan of imaging parallel to the hard palate from the maxillary sinus base to the frontal sinus roof. The scanning time was 10-12 seconds. The mean radiation exposure dose was 34.0 mGy. The images were transferred to the "picture archiving and communicating system" -PACS (Eroglu, Eskisehir). All images were evaluated in a separate workstation (Philips Medical Systems, the Netherlands) connected to the picture archiving and communicating system (PACS), where the image manipulations, such as window setting, magnification, and measurement, could be performed. In all cases, coronary and sagittal reformat images were created. According to these protocols, anatomic variations in CT sections were evaluated in both bone (window width: 2000 Hounsfield unit (HU), window level: 350 HU) and soft tissue (window width: 200 HU, window level: 40 HU) windows.

Paranasal sinus CTs were evaluated concerning the septum deviation, septal spur, pneumatized septum, concha bullosa (CB) and types, secondary middle turbinate, paradoxical middle turbinate, uncinate agenesis, uncinate duplication, uncinate bulla, atelectatic uncinate process (UP), bifid UP, agger nasi cell, Haller cell , ethmoid bulla and giant eth-

moid bulla, frontoethmoidal cells (Type 1, Type 2, Type 3, Type 4), supraorbital ethmoid cell (SOEC), level differences of ethmoid roof (according to Keros classification), maxillary sinus hypoplasia, frontal sinus hypoplasia and aplasia, Onodi cell, pterygoid process pneumatization (PPP), vidian nerve (VN) protrusion, sphenoid large wing pneumatization (CLWP), maxillary nerve (MN) protrusion, anterior clinoid process pneumatization (ACPP), sphenoid sinus-internal carotid artery (ICA) relationship, sphenoid sinus and optic nerve (ON) relationship.

In our study, PPP was accepted as the extension of pneumatization beyond the most inferolateral surface of VN in the horizontal plane. We defined CLWP as a pneumatization extending beyond a line crossing the foramen rotundum or extending beyond MN in the vertical plan. The presence of air around the VN and MN was accepted as an indicator of VN and MN protrusion. ON and ICA protrusions were accepted as any degree of protrusion of these structures towards the sphenoid sinus cavity. We evaluated the CB by accepting any degree of pneumatization as significant. We have described the paradoxical turbinate as a condition that can be traced in two consecutive images of the coronal section, although not paradoxical at other levels.

Statistics Analysis

Descriptive analysis was performed to obtain information about the general characteristics of the study groups. Continuous variables were given as mean±standard deviation, and categorical variables were given as numbers and percentages. In the comparison between the groups, the Student t-test was used for the parameters that fit the normal distribution. All statistical data were analyzed using SPSS 21.0 package program. The data obtained were coded and transferred to the computer program.

Results

Of the 300 patients, 151 were male (47.2%), and 169 were female (52.8%). The mean age was 39.8±15.8 years. The most common anatomic variation was the agger nasi cell, with 86.3% (n=276). The least detected anatomical variations were pneumatized inferior concha and bifid inferior concha with 0% (n=0), inferior concha hypoplasia with 0.3% (n=1), and bifid uncinate process variations with 0.6% (n=2). The breakdown of anatomic variations of our cases by CT is presented in Table 1.

The incidence of septum deviation (SD) was 72.8% (n=233). Of 233 patients with SD, 10.3% (n=24) were bilateral ("S") and 89.7% (n=209) were unidirectional ("C chaped"). Con-

Table 1. Distribution of anatomical variations of cases

Anatomical variation	Number (n=320)	Percentage (%)
Septum deviation	233	72.8
Bone spur in the septum	140	43.8
Pneumatized septum	8	2.5
Concha bullosa (medium)	243	75.9
Paradoxical middle turbinate	53	16.6
Secondary middle turbinate	6	1.9
Paradoxical inferior turbinate	24	7.5
Lower turbinate hypoplasia	1	0.3
Frontoetmoid cell	167	52.2
Atelectatic uncinate process	8	2.5
Bifid uncinate process	2	0.6
Uncinate bulla	37	11.6
Giant ethmoid bulla	38	11.9
Maxillary sinus hypoplasia	26	8.1
Agger nasi cell	276	86.3
Haller cell	88	27.5
Supraorbital ethmoidal cell	19	5.9
Onodi cell	81	25.3
Frontal sinus aplasia	18	5.6
Frontal sinus hypoplasia	26	8.1
Pterygoid process aeration	141	44.1
Vidian nerve protrusion	141	44.1
Anterior clinoid process aeration	92	28.8
Optic nerve protrusion	91	28.4
Internal carotid artery protrusion	105	32.8
Internal carotid artery dehiscence	24	7.5
Sphenoid large wing aeration	69	21.9
Maxillary nerve protrusion	69	21.6

Figure 1. CT scans of different patients; **(a)** In the coronal plane, a unidirectional 'C' shaped left SD and septal spur extending to the lateral nasal wall at the middle meatus level on the same side. **(b)** Axial CT shows septal spur narrowing the nasal cavity (arrows). **(c)** Coronal CT shows the pneumatization of the septum in the posterosuperior section of the nasal septum. **(d)** Bilateral vertical lamellar type concha bullosa (straight arrows) and left pneumatized uncinate process (dashed arrow). **(e)** Bilateral inferior bullous type and **(f)** Bilateral extensive (true) type concha bullosa (straight arrows).

Table 2. Frequency of concha bullosa (middle) types

Concha bullosa (middle) types	Unilateral %	Bilateral %	Total %
Vertical lamellar	33.3	35.8	69.1
Inferior bullous	5.3	2.5	7.8
Extensive (real)	12	11.1	23.1
Total	50.6	49.4	100

comitant septal spur was detected in 54.5% (n=127) of 233 patients with SD (Fig. 1a, b). In our study, 43.8% (n=140) of the patients had bone spur in the nasal septum. In our study, the incidence of septum pneumatization was 2.5% (n=8) (Fig. 1c).

In our study, all pneumatization forms of the middle turbinate were accepted as CB, and total CB was found to be 75.9% (n=243). Of the 243 patients with CB, 69.1% were vertical lamellar, 23.1% were extensive (true), and 7.8% were inferior bullous type (Fig. 1d–f). 50.6% of our patients had unilateral, and 49.4% had bilateral CB. The most common vertical lamellar type CB was seen both unilaterally and bilaterally (Table 2).

The frequency of the paradoxical middle turbinate was found to be 16.6% (n=53). 22.6% of these cases were bilateral (Fig. 2a). In our study, the rate of secondary middle turbinate was found to be 1.9% (n=6). 83.3% of these cases were symmetrical (Fig. 2c, d). In addition, unilateral inferior
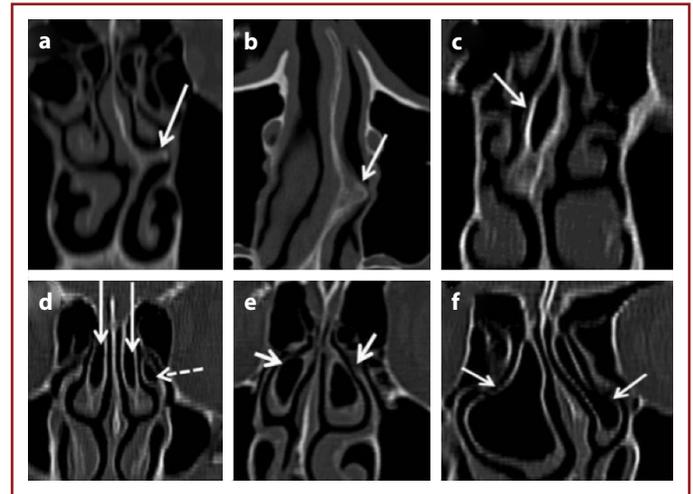
turbinate hypoplasia was detected in one patient (0.3%) (Fig. 2d–f). The paradoxical inferior turbinate was found to be 7.5% (n=24) (Fig. 2g). In all of these cases, the paradoxical turbinate was unilateral.

The frequency of frontoethmoidal cells was 52.2% (n=167 cases). In 167 cases with frontoethmoidal cells, the typing was evaluated in both directions (275). Accordingly, type 1 (most common) frontoethmoidalcells were detected in 60%, type 2 in 23.3%, type 3 in 12.7% and type 4 (most rare) frontoethmoidal cells in 4% (Fig. 3) (Table 3).

CL-ethmoid roof elevation relationships were mostly symmetrical (75.9%), and the most common Kerosus type 2 was 66.1% (n=423) (Table 4).

Anatomic variations that we have never encountered (0% (n = 0)) were UP agenesis and inferior turbinate variations (bifid inferior turbinate and inferior turbinate bullosa), which were reported to be also rare in the literature.
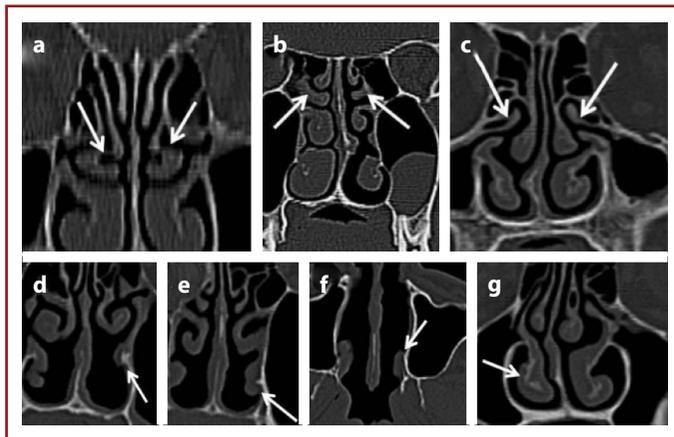
Figure 2. CT scans of different patients; **(a)** The bilateral paradoxical middle turbinate in the coronal plane (arrows). **(b)** Concha (arrows) narrowing the OMU is seen in bilateral middle turbinate posterosuperior in coronal CT and **(c)** in the axial CT in the lateral neighborhood of the bilateral middle turbinate (arrows). **(d)** and **(e)** Coronal CT shows hypoplasia of the left lower turbinate in successive sections and **(f)** in the axial section. **(g)** Coronal CT shows a paradoxical inferior turbinate (arrow) on the right.
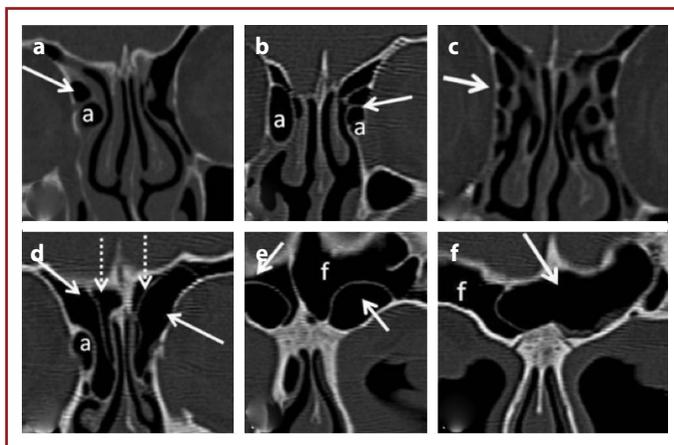

Figure 3. Coronal CT sections of different patients; **(a)** Type 1 frontoethmoid cell. On the right is a single-cell (arrow) on the agger nasi cell (a). **(b)** and **(c)** Type 2 frontoethmoid cells. On the agger nasi cell (a), several cells (straight arrows) are seen on the left and the right. **(d)** and **(e)** Type 3 frontoethmoid cells. Sequential sections show bilateral single-cells (arrows) that can be selected on the right agger nasi cell (a), markedly narrowing the frontal recess (dotted arrow) and extending into the frontal sinus. **(f)** Coronal CT shows type 4 frontoethmoid cells on the left, all located within the frontal sinus (f).

Discussion

CB is one of the most common variations of the paranasal sinuses, and its frequency varies between 14-80% in the literature. The reason for this proportional difference is the variation in the pneumatization criteria used in the studies [7,8]. In our study, all formations of the middle turbinate were accepted as CB and consistent with the literature, a total of 75.6% (n=242) CB was determined. Pneumatization

Table 3. Frequency of frontoethmoid cell types

Frontoetmoid (Kuhn) cell classification	Total number (n=167)	Percentage (%)
Type 1 (single-cell)	165	60
Type 2 (multiple stratified cells)	64	23.3
Type 3 (single-cell extending into the frontal sinus)	35	12.7
Type 4 (single-cell completely within the frontal sinus)	4	11

Table 4. KL-ethmoid roof height relations according to Keros classification

	Right (n)	Left (n)	Bilateral	Total n (%)
Keros 1	29	23	58	168 (26.2)
Keros 2	38	39	173	423 (66.1)
Keros 3	10	15	12	49 (7.7)

of the inferior turbinate is an extremely rare condition and can be detected incidentally during radiological evaluation [9–11]. We think that the reason why it is common that the lower turbinate, unlike the other turbinates, is not an extension of the ethmoid bone but a separate bone structure in itself. In some cases, the large nasolacrimal duct may give the impression of inferior turbinate pneumatization. It is essential to distinguish these cases well [12]. Inferior CB was not detected in our study.

The paradoxical turbinate is clinically irrelevant if it is small. Although it is not a predisposing factor alone, it is considered to be important in the etiology of sinusitis if it is very large and in combination with other anatomical variations [13]. The secondary middle turbinate is a rare variation. During the endoscopic nasal examination, it may be mistaken for polyp or osteoma. It can also be confused with curved UP [12]. It may predispose to infectious sinus disease by narrowing the OMU [14]. Thus, it is important that they are recognized and reported on CT.

In our study, the anatomic variations that we never encountered (0% (n=0)) were UP agenesis and inferior turbinate variations, which were reported to be rare in the literature. The variations of the lower turbinate are seen in 2% of the population and may cause complaints, such as nasal obstruction and atypical headache. Yasan et al.[12] reported a 0.1% incidence of bifid inferior turbinates.

Currently, the frontal recess is the key to endoscopic frontal sinusotomy [15]. Since the imaging of the frontal recess with axial CT scans is difficult, it should be supported by

sagittal reconstruction. Because of the configuration of the frontoethmoid cells, the agger nasi cell must be explored first to approach the frontal recess in operation. All of these cells are located above the agger nasi cell. Type 1, type 2 and type 3 frontoethmoid cells need to be removed to reach frontal recess and supply frontal drainage [13].

The Agger nasi cells may bring on frontal sinus pathologies, by causing constriction of frontal recess in association with the size and location [16]. They may also bring about epiphora, dacryocystitis, and visual symptoms due to the adjacent lacrimal fossa located laterally [17]. Due to all these features, Agger nasi cells can be considered as a key to understanding the complex anatomical configuration of the frontal recess [18] (Fig. 4a–c). They are the most commonly removed cells in endoscopic sinus surgery (ESS) applications [19,20].

The Haller cell also increases the risk of orbital injury during ESS, particularly in cases of over-pneumatization [21]. The Haller cell is usually diagnosed by CT, and endoscopic diagnosis is often unlikely [20] (Fig. 4d–f).

SOEC is located in the superior and medial part of the orbita and is important because they will disrupt surgical field sterilization when opened, especially when approached to the skull base with anterior cranial fossa approach (Fig. 5a). SOEC is located anterior to the anterior ethmoidal artery. Therefore, the anterior ethmoid artery may be damaged if the SOEH is opened by a posterior approach [22]. EMD is a rare variation and may coexist with maxillary sinus hypoplasia [23]. Before ESS, awareness of the presence of EMD may be important to prevent the surgeon from losing its anatomic orientation during the operation and experiencing stress.
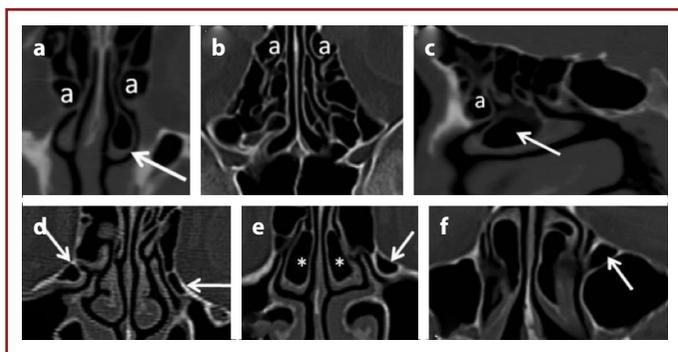
The Onodi cell is located between the anterior cranial fossa and the sphenoid sinus in the inferomedial region of the ON (Fig. 5b,c). The ON canal can sometimes pass through the Onodi cell, especially if ACPP is present. Especially after posterior ethmoidectomy, ON may be damaged if no Onodi cell is detected during entry into the sphenoid sinus [22]. The presence of Onodi cells before surgery will significantly reduce the risk of complications because of their proximity to important structures, such as ON, and less frequently ICA [24]. The Onodi cell may also cause the sphenoidotomy to fail because certain points (optic nerve and carotid artery) that are traditionally associated with the sphenoid are seen in the posterior ethmoid, and the surgeon may be mistaken by burning in such a situation, it enters the sphenoid sinus [25].

The frontal sinus is the most common sinus with aplasia and hypoplasia. Detection of this variation by CT is particularly important given that the absence of frontal sinus pneumatization by conventional radiographs prevents the accidental interpretation of frontal sinus pathology (Fig. 5d,e).

When the ethmoid roof level is low, the risk of intracranial penetration (brain damage, bleeding) during surgery is considerably very high, and any damage to the bone structure, which is too thin in this area, may result in CSF leakage and recurrent meningitis in the postoperative period. In addition, anterior ethmoidal artery injury may cause severe bleeding into the orbita [20]. Asymmetry at the height of the ethmoid roof, differences in the depth and width between olfactory fossas may also cause unwanted surgical
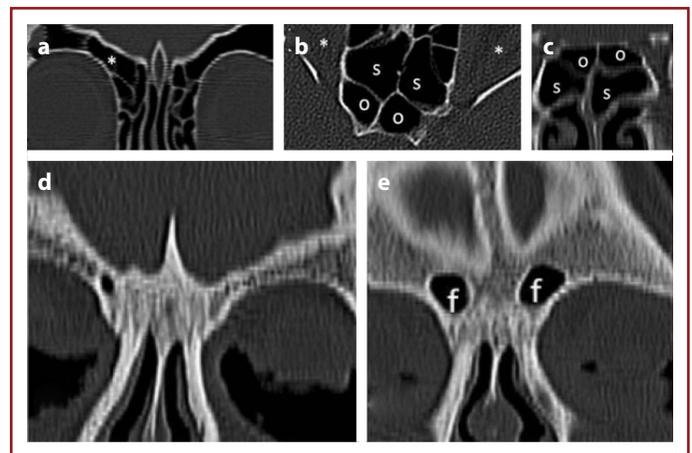

Figure 4. (a) Coronal **(b)** axial and **(c)** sagittal CT sections passing through the anterior to the middle turbinate of the same patient show agger nasi cells (a) medial neighborhood to bilateral orbita. There is also a variation of the middle turbinate bullosa on the left (arrow). **(d)** The coronal CT section shows Haller cells (arrows) adjacent to the inferomedial to the bilateral orbita. In another case, it was noted that Haller cell (arrow) narrowed the infundibulum with maxillary sinus ostium, followed by **(e)** coronal and **(f)** axial CT on the left. It is also accompanied by bilateral middle BP (asterisk).

Figure 5. (a) Coronal CT shows a supraorbital ethmoid cell (asterisk) located in the superior orbita on the right cross-section of the anterior to the middle turbinate. **(b)** Onodi cell (o) adjacent to the optic nerve (asterisk) medial on axial CT, located between the anterior cranial fossa and the sphenoid sinus (s), is seen. **(d)** bilateral frontal sinus aplasia and **(e)** bilateral frontal sinus hypoplasia **(f)** are observed in different cases.

trauma. This asymmetry should also be indicated in radiological reporting [13,26].

It is important to recognize the septal deviations because in case of severe deviation, they may cause compression of the middle turbinate and obstruction in the middle meatus. In this case, they may restrict the endoscopic image and complicate surgical intervention [17].

Atelectatic UP is usually associated with hypoplasic opacified maxillary sinus [27,28]. In our study, the frequency of atelectatic UP was found to be 2.5% (n=8), and in all of these cases, it was found that maxillary sinus hypoplasia was present on the side with atelectatic UP (Fig. 6a). This variation is very important in cases that will undergo anterior ESC. If it is not defined radiologically, it may lead to significant complications during unsinectomy, which poses a great danger to the orbital and optic nerve. This variation and associated sinus hypoplasia must be defined by the radiologist [13,29]. Maxillary sinus hypoplasia (MSH) is rare, sometimes mistakenly interpreted as chronic sinusitis [30]. With MSH, the orbita may be low-set and is more vulnerable to injury during the surgery. Preoperative knowledge of severe sinus hypoplasia and associated hypoplasic UP, if any, will reduce the risk of orbital penetration during ESC [31]. The findings showed that 30.8% (n=8) of the patients with maxillary sinus hypoplasia were accompanied by UP atelectasis on the same side (Fig. 6b).

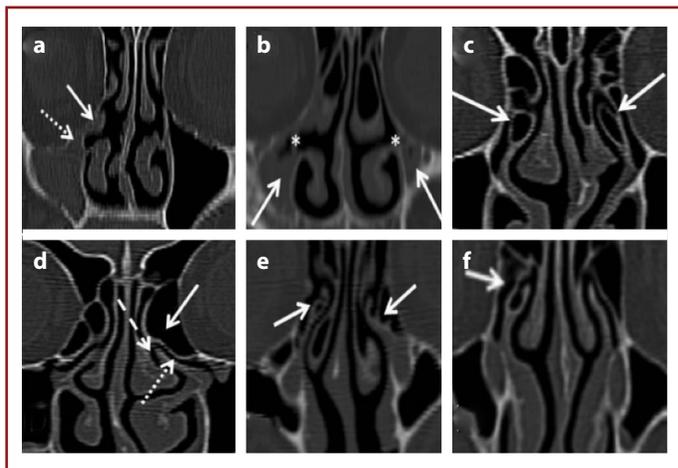Uncinate bulla increases the width of the uncinate, thus

Figure 6. CT scans of different patients; **(a)** Coronal CT shows that the opacified hypoplastic maxillary sinus antrum (dotted arrow) and UP (straight arrow) are attached to the orbital inferomedial. **(b)** Bilateral hypoplastic maxillary sinus (straight arrow) and UP atelectasis (asterisk) are seen. **(c)** Bilateral uncinate bulla (straight arrow) variation and narrowing of the ostiomeatal complex are observed. **(d)** On the left is an extremely pneumatized ethmoid bulla (straight arrow) that narrows the middle meatus (dashed arrow) and infundibulum (dotted arrow). Coronal CT shows **(e)** bilateral and **(f)** right bifid UP (straight arrow).

posing a potential danger to the infundibulum [23] (Fig. 6c). As in the combination of uncinate bulla and Haller cell, the pathogenic effect that may occur in the coexistence of certain anatomical variations is also higher than that of the individual effect [14]. Ethmoid bulla is a reliable surgical cue point because it is the largest and most stable of the anterior ethmoid cells. Giant ethmoid bulla may cause recurrent sinusitis by narrowing the middle meatus and infundibulum [32] (Fig. 6d). In our study, 0.6% (n=2) bifid UP was detected, and bilateral bifid UP was detected in one of the cases (Fig. 6e, f). Due to its rarity in the literature, the bifid UP, which we determined in our study, has become crucial.

Sphenoid sinus surgery is riskier than other sinus surgeries due to the presence of vital organs in the vicinity [33]. As sphenoid sinus pneumatization increases, it is stated that ICA and OS project on the lateral wall of the sinus [2]. In an area where the anatomy is so variable, it is very important to have knowledge before the surgery [34].

The presence of PPP is an important way of accessing the center of the skull base. For example, an extended transnasal endoscopic approach can be used to achieve a pterygoid process. These techniques may be important in preoperative planning by providing a route for the endoscopic repair of CSF leakage and endoscopic biopsy of skull base lesions.

There is a variable relationship between the Vidian canal and the sphenoid sinus, and VS is known to cause a clinical syndrome (Vidian neuralgia) characterized by deep pain in the nasal cavity. Radiological prediction of the relationship between the Vidian canal and the sphenoid sinus will reduce the risk of complications in endoscopic transsphenoidal and vidian neurectomy surgery [33].

ON may pass through the sphenoid sinus, especially when an ACPP is present [35,36]. In case of protrusion of the ON into the sphenoid sinus, injury to the ON may result from a surgical trauma or inflammatory sinus disease. ON compression may lead to ischemia and venous congestion of the nerve [33]. The risk of blindness is very high if the surgeon damages the optic nerve [37]. Recent studies have re-emphasized the need for multiplanar reconstruction in the preoperative practice of this complex anatomical region [38].

Occasionally, ICA may protrude into the sphenoid sinus, especially in cases of excessive pneumatization of the sphenoid sinus. The dehiscence of the bone structure on the artery causes the artery to come into direct contact with the sinus mucosa and can be confused with pathological soft tissues if a careful radiological examination is not performed. Failure to have knowledge of preoperative

ICA protrusion and/or dehiscence may result in ICA injury and fatal bleeding, which is difficult to control. In addition, sphenoid sinus infection in the presence of protrusion and dehiscence may cause ICA damage [33]. The intersphenoid septum, which divides the sinus into two, is usually folded to one side and adheres to the bone wall covering the ICA. This part may undergo avulsion during surgery [17,39]. To avoid bone septum fracture during surgery, the surgeon must know the septa-related ICA, if any [36].

In the presence of protruding MS, there is a possibility of iatrogenic nerve damage during ESC [40]. Furthermore, due to their association with the maxillary nerve, sphenoid sinusitis may cause trigeminal neuralgia [39].

Conclusion

CT is a gold standard imaging method used routinely for the detection of sinonasal anatomy and pathologies. Routine examination of sinonasal CT images in 3 planes is important. Multiplanar reformatted images in the sagittal and coronal planes are particularly helpful. In fact, it is not possible to fully evaluate the anatomy without resorting to these reformatted images. With the advantages of multidetector CT technology, optimal images can be obtained by shortening the scanning time with high resolution and speed without disturbing patient comfort. Coronal and sagittal reconstructions obtained from single and axial thin sections provide great advantages in evaluating anatomy. Optimal transfer of anatomic variations and pathologies to the surgeon before ESC is essential for the selection of the correct surgical method and the safe application of the surgery.

In this study, a significant portion of the determined variations (such as ICA protrusion and dehiscence, ethmoid roof asymmetry, Onodi cell, atelectatic UP) may cause significant complications during the surgery in case they are not determined before the surgery, some of these complications (such as uncinate bulla, agger nasi, Haller cell, giant ethmoid bulla) are predisposant factors to mucociliary drainage and aeration problems. Therefore, it is important to know and define the appearance of these variations on CT. In our study, significant variation was observed in the sinonasal region, and it was once again emphasized that paranasal sinus CT was very valuable in determining these variations.

References

1. Warwick R, Williams PL. Gray's Anatomy. 35th British ed. Philadelphia, W.B. Saunders; 1973.
2. Kaya M, Çankal F, Gumusok M, Apaydin N, Tekdemir I. Role of anatomic variations of paranasal sinuses on the prevalence of sinusitis: Computed tomography findings of 350 patients. Niger J Clin Pract 2017;20:1481–8. [CrossRef]
3. Önerci M. Endoskopik Sinüs Cerrahisi. 2nd ed. Ankara: Kutsan Ofset, 1999: 1–24.
4. Elwany S, Medanni A, Eid M, Aly A, El-Daly A, Ammar SR. Radiological observations on the olfactory fossa and ethmoid roof. J Laryngol Otol 2010;124:1251–6. [CrossRef]
5. Dasar U, Gokce E. Evaluation of variations in sinonasal region with computed tomography. World J Radiol 2016;8:98–108.
6. Kaplan Y, Müderris S, Kunt T. Tomographic Analysis of Sinonasal Variations and Relationship with Sinusitis . [Article in Turkish]. C.Ü. Tıp Fakültesi Dergisi 2004;26:29–36.
7. Zeinreich S, Albayram S, Benson ML, Oliveiro P. The ostiomeatal complex and functional endoscopic surgery. In: Som P, editors. Head and Neck Imaging. 4th ed. St Louis: Mosby, 2003; 149–73.
8. Jones NS. CT of the paranasal sinuses: a review of the correlation with clinical, surgical and histopathological findings. Clin Otolaryngol Allied Sci 2002;27:11–7. [CrossRef]
9. Kayalioglu G, Oyar O, Govsa F. Nasal cavity and paranasal sinus bony variations: a computed tomographic study. Rhinology 2000;38:108–13.
10. Dogru H, Doner F, Uygur K, Gedikli O, Cetin M. Pneumatized inferior turbinate. Am J Otolaryngol 1999;20:139–41. [CrossRef]
11. Kharoubi S. [Pneumatization (concha bullosa) of the inferior turbinate: case report and literature review]. Rev Laryngol Otol Rhinol (Bord) 2010;131:321–4.
12. Yasan H, Aynali G, Akkuş O, Yarıktaş M, Doğru H, Baykal B, et al. Alt konka anatomik varyasyonlarının sıklığı. KBB Forum 2006;5:12–4.
13. Beale TJ, Madani G, Morley SJ. Imaging of the paranasal sinuses and nasal cavity: normal anatomy and clinically relevant anatomical variants. Semin Ultrasound CT MR 2009;30:2–16.
14. Kantarci M, Karasen RM, Alper F, Onbas O, Okur A, Karaman A. Remarkable anatomic variations in paranasal sinus region and their clinical importance. Eur J Radiol 2004;50:296–302. [CrossRef]
15. Gümüs C, Yıldırım A, Erdinc P, Öztoprak B, Karaman B. Presence of Frontal Cell in Frontal Sinusitis And Its Association With Anatomic Variations. C.Ü. Tıp Fakültesi Dergisi 2005;27:69–73.
16. Huang BY, Lloyd KM, DelGaudio JM, Jablonowski E, Hudgins PA. Failed endoscopic sinus surgery: spectrum of CT findings in the frontal recess. Radiographics 2009;29:177–95. [CrossRef]
17. Cashman EC, Macmahon PJ, Smyth D. Computed tomography scans of paranasal sinuses before functional endoscopic sinus surgery. World J Radiol 2011;3:199–204. [CrossRef]

18. Wormald PJ. The agger nasi cell: the key to understanding the anatomy of the frontal recess. Otolaryngol Head Neck Surg 2003;129:497–507. [CrossRef]

19. Chong VF, Fan YF, Lau D, Sethi DS. Functional endoscopic sinus surgery (FESS): what radiologists need to know. Clin Radiol 1998;53:650–8. [CrossRef]

20. Tan HM, Chong VFH. CT of the paranasal sinuses: normal anatomy, variants and pathology. CME Radiol 2001;2:120–5.

21. Sahin C, Yılmaz YF, Titiz A, Ozcan M, Ozlugedik S, Unal A. The Anatomic Variations of Paranasal Sinuses: Computerized Tomography Study. [Article in Turkish]. KBB ve BBC dergisi 2007;15:71–3.

22. Arslan H, Aydinlioğlu A, Bozkurt M, Egeli E. Anatomic variations of the paranasal sinuses: CT examination for endoscopic sinus surgery. Auris Nasus Larynx 1999;26:39–48. [CrossRef]

23. Rao VM, el-Noueam KI. Sinonasal imaging. Anatomy and pathology. Radiol Clin North Am 1998;36:921–39. [CrossRef]

24. Thanaviratananich S, Chaisiwamongkol K, Kraitrakul S, Tangsawad W. The prevalence of an Onodi cell in adult Thai cadavers. Ear Nose Throat J 2003;82:200–4. [CrossRef]

25. Keast A, Yelavich S, Dawes P, Lyons B. Anatomical variations of the paranasal sinuses in Polynesian and New Zealand European computerized tomography scans. Otolaryngol Head Neck Surg 2008;139:216–21. [CrossRef]

26. Bayram M, Sirikci A, Bayazit YA. Important anatomic variations of the sinonasal anatomy in light of endoscopic surgery: a pictorial review. Eur Radiol 2001;11:1991–7. [CrossRef]

27. Landsberg R, Friedman M. A computer-assisted anatomical study of the nasofrontal region. Laryngoscope 2001;111:2125–30. [CrossRef]

28. Branstetter BF 4th, Weissman JL. Role of MR and CT in the paranasal sinuses. Otolaryngol Clin North Am 2005;38:1279–99. [CrossRef]

29. Valvassori GE, Mafee MF, Carter B. Nasal Cavity and Paranasal Sinuses. Imaging the Head and Neck. New York: Thieme; 1995:15:248–329.

30. Kumar H, Choudhry R, Kakar S. Accessory maxillary ostia: topography and clinical application. J Anat Soc India 2001;50:3–5.

31. Evans JJ, Hwang YS, Lee JH. Pre-versus post-anterior clinoidectomy measurements of the optic nerve, internal carotid artery, and opticocarotid triangle: a cadaveric morphometric study. Neurosurgery 2000;46:1018–21. [CrossRef]

32. Zinreich SJ. Functional anatomy and computed tomography imaging of the paranasal sinuses. Am J Med Sci 1998;316:2–12. [CrossRef]

33. Sirikci A, Bayazit YA, Bayram M, Mumbuc S, Gungor K, Kanlikama M. Variations of sphenoid and related structures. Eur Radiol 2000;10:844–8. [CrossRef]

34. Elwany S, Elsaeid I, Thabet H. Endoscopic anatomy of the sphenoid sinus. J Laryngol Otol 1999;113:122–6. [CrossRef]

35. Lim CC, Dillon WP, McDermott MW. Mucocele involving the anterior clinoid process: MR and CT findings. AJNR Am J Neuroradiol 1999;20:287–90.

36. Abdullah BJ, Arasaratman S, Kumar G, Gopala K. The Sphenoid Sinuses: Computed Tomographic Assessment of Septation, Relationship to the Internal Carotid Arteries, and Sidewall Thickness in the Malaysian Population. J HK Radiol 2001;4:185–8.

37. Maniglia AJ. Fatal and major complications secondary to nasal and sinüs surgery. Laryngoscope 1989;99:276–83. [CrossRef]

38. Lee KJ. Essential Otolaryngology Baş ve Boyun Cerrahisi. 8.baskı. Ankara: Güneş kitabevi; 2004:388–410.

39. Dwivedi AND, Singh KK. CT of the paranasal sinuses: normal anatomy, variants and pathology. Journal of Optoelectronics and Biomedical Materials 2010;2:281–9.

40. Hewaidi G, Omami G. Anatomic Variation of Sphenoid Sinus and Related Structures in Libyan Population: CT Scan Study. Libyan J Med 2008;3:128–33. [CrossRef]